Scattering Pattern Measurement and Analysis of Sputtered-Glass Optical Waveguides for Integrated Optics

MASAAKI IMAI, MEMBER, IEEE, YOSHIHIRO OHTSUKA, AND MAMORU KOSEKI

Abstract—The radiation patterns from optical waveguides prepared by sputtered 7059 glass thin film onto pyrex glass substrates are measured in order to clarify the loss mechanisms producing the scattering. The angular distributions of the scattered light can be explained by the presence of its surface roughness at film-substrate and film-air interfaces and/or of bulk inhomogeneities of the waveguide core. For waveguides with a relatively high loss of several dB/cm, for example, the patterns are consistent with the theory based on a cross-correlated model of these imperfections, assuming correlation lengths of the order of 0.1λ in the normal direction and of the same order as the wavelength λ in the parallel direction to the waveguide. The rms value of surface roughness to that of bulk inhomogeneities divided by λ is also determined by comparing the measured scattering curves with the theoretically calculated curves.

I. Introduction

SCATTERING light from a thin-film optical waveguide represents a loss mechanism and, in addition, such scattering can limit the performance of integrated optical devices. In particular, the dynamic range obtainable in integrated optical signal processing devices such as spectrum analyzers is expected to degrade its characteristics by the waveguide scattering. In-plane scattering actually leads to the performance degradation of the integrated spectrum analyzer [1]. On the other hand, out-of-plane scattering is found to yield valuable diagonostic information of the waveguide imperfections. A knowledge of scattering in optical waveguides is useful in optimizing the waveguide fabrication procedure to reduce scattering to a minimum. In order to attain this, it is necessary to have some understanding of the mechanisms producing a scattering loss.

The effect of the scattering on radiation loss and mode conversion of the guided beam has been studied so far for a thin-film optical waveguide in which scattering may originate from roughness on the waveguide or substrate surfaces [2]-[4], or from index inhomogeneities of the waveguide core region [5]-[7]. These imperfections cannot exist independently from each other for the sputtered glass waveguide and are greatly affected by surface preparation techniques and sputtering conditions [8]. Recently, the theory of scattering in thin-film waveguides was extensively developed by Miyanaga *et al.* [9], which is required for comparison with the measurements reported here. The theory represents the calculation of angular distributions of out-of-plane scattered intensity in the presence of mutual correlation between surface roughness and bulk inhomogeneities.

In the present work, measurement and analysis on sputtered Corning 7059 glass thin film onto pyrex glass substrates will be described in order to estimate quantitatively the fine structures within the waveguide component. The radiation patterns of the optical waveguide may be related to size distributions and densities in a statistical manner, as is the case of light scattering from particles in bulk systems. The statistical properties of the sputtered glass waveguide can be analyzed by comparing the measured scattering curves with the theoretically calculated curves, and the parameters matching those of the experimental data are determined graphically.

II. Theory and Numerical Analysis

The details of the theory of waveguide scattering have been discussed elsewhere [9], so that only the results are presented here in order to help understand the theoretical development. The waveguide to be discussed is a thin-film waveguide consisting of three layers: air, thin film (waveguide core), and a substrate with the refractive indexes of n_1, n_2, and n_3, respectively. As shown in Fig. 1, the waveguide is assumed to include surface roughness at film-substrate and film-air interfaces as well as bulk inhomogeneities in the waveguide core. It is also assumed that the imperfect waveguide is connected to an ideal system at $z = 0$ and $z = L$. These waveguide imperfections are mathematically described by the square of the index

$$n^2(x, z) = n_i^2 + \Delta n_w^2(x, z) + \Delta n_r^2(x, z) \tag{1}$$

where the first term $n_i^2 (i = 1, 2, 3)$ is the squared index in each region and the second term $\Delta n_w^2(x, z)$ represents a geometrical deviation from perfect shape and is given by

$$\Delta n_w^2(x, z) = \begin{cases} n_2^2 - n_1^2; & x \geqq 0 \text{ and } x \leqq f(z) \\ n_1^2 - n_2^2; & x \leqq 0 \text{ and } x \geqq f(z) \\ n_3^2 - n_2^2; & x \geqq -t \text{ and } x \leqq -t + g(z) \\ n_2^2 - n_3^2; & x \leqq -t \text{ and } x \geqq -t + g(z) \\ 0; & \text{elsewhere.} \end{cases} \tag{2}$$

Manuscript received September 2, 1981; revised November 19, 1981. This work was supported in part by a Scientific Research Grant-in-Aid from the Ministry of Education, Science, and Culture, Japan.

M. Imai and Y. Ohtsuka are with the Department of Engineering Science, Hokkaido University, Sapporo, Japan.

M. Koseki was with the Department of Engineering Science, Hokkaido University, Sapporo, Japan. He is now with the Totsuka Works, Hitachi Limited, Yokohama, Japan.

0018-9480/82/0400-0635$00.75

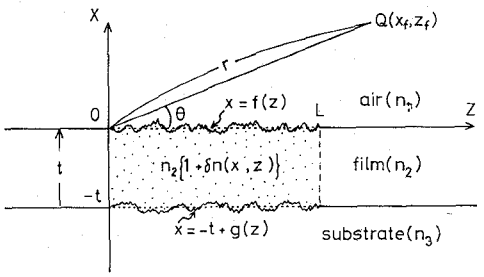

Fig. 1. Coordinate system of a thin-film waveguide with waveguide surface roughness and waveguide core inhomogeneities.

In addition, the third term $\Delta n_r^2(x, z)$ in (1) denotes the index fluctuations in the waveguide core:

$$\Delta n_r^2(x,z) = \begin{cases} 2n_2^2 \delta n(x,z); & -t \leqq x \leqq 0 \\ 0; & \text{elsewhere.} \end{cases} \tag{3}$$

The random functions $f(z)$, $g(z)$, and $\delta n(x, z)$ used in the expressions obey the following statistical restrictions:

$$|\delta n(x,z)| \ll 1, \langle \delta n(x,z) \rangle = 0$$

$$\langle \delta n(x_1, z_1)\, \delta n(x_2, z_2) \rangle = V^2 \exp\left\{ -\frac{|x_1 - x_2|}{a_x} - \frac{|z_1 - z_2|}{a_z} \right\}$$

$$|f(z)|, |g(z)| \ll t, \langle f(z) \rangle = \langle g(z) \rangle = 0$$

$$\langle f(z_1) f(z_2) \rangle = \langle g(z_1) g(z_2) \rangle = V_f^2 \exp\left\{ -\frac{|z_1 - z_2|}{b_z} \right\} \tag{4}$$

$$\langle f(z_1) g(z_2) \rangle = V_f^2 \exp\left\{ -\frac{t}{b_x} - \frac{|z_1 - z_2|}{b_z} \right\}$$

$$\langle \delta n(x_1, z_1) f(z_2) \rangle = V V_f \exp\left\{ -\frac{|x_1|}{d_x} - \frac{|z_1 - z_2|}{d_z} \right\}$$

$$\langle \delta n(x_1, z_1) g(z_2) \rangle = V V_f \exp\left\{ -\frac{|x_1 + t|}{d_x} - \frac{|z_1 - z_2|}{d_z} \right\}$$

where the angle bracket stands for an ensemble average and V, V_f are the standard deviations of $\delta n(x, z)$, $f(z)$ [or $g(z)$], respectively. a, b, and d in the exponential functions represent the correlation lengths. The last two equations in (4) refer to a cross correlation function between surface roughness and bulk inhomogeneities. For the sake of convenience, we assume a positive cross correlation since both the surface roughness and the bulk inhomogeneities may be related to the same imperfections in the sputtering process [4].

These imperfections can produce the scattered light in the waveguide. It is possible to express the scattered electric field in a perturbation form as

$$E_y(x,z) = E_y^0(x,z) + \delta E_y(x,z), (|\delta E_y(x,z)| \ll |E_y^0(x,z)|) \tag{5}$$

where $E_y^0(x, z)$ is the unperturbed field of an incident TE_0 mode, and $\delta E_y(x, z)$ represents the perturbation term. The perturbed electric field can be obtained by using the Green's function method [6] and is expressed by the expansion

$$\delta E_y^{(\pm)}(x,z) = \sum_m A_m^{(\pm)}(z)\, E_m(x,z) + \sum_{i=1}^{2} \int_0^{n_3 k} C_\alpha^{(\pm)}(z,\beta)\, E_\alpha(x,z,\beta)\, \frac{\beta}{\rho}\, d\beta \tag{6}$$

where k is the wavenumber in vacuum and β, ρ are the propagation constants. The first summation extends over all guided modes $E_m(x, z)$ of the discrete spectrum. The integral extends over all radiated modes $E_\alpha(x, z, \beta)$ of the continuum, and the summation sign in front of the integral indicates the two degenerate modes of air radiation [10]. The superscript plus and minus signs denote coupling into the forward and backward scattering waves. The expansion coefficients $A_m^{(\pm)}(z)$ and $C_\alpha^{(\pm)}(z, \beta)$ are an unknown function of z, but are easily obtained by use of orthogonality relations and normality properties for eigenmodes of guided and radiation modes. Substituting the proper form for each mode in (6), the scattered electric field can be evaluated. We assume that observation point $Q(x_f, z_f)$ is sufficiently far from the waveguide. This fact permits us to take the air mode for radiation in the air region and both the air and substrate modes for radiation in the substrate region. Based on a stationary method, the time-averaged power passing through the unit area perpendicular to $\overline{OQ}$ is obtained from the definition of the pointing vector. The time-averaged power is given by an ensemble averaged form

$$\langle P^{(\pm)}(\theta) \rangle = \frac{n_1 k}{2\omega\mu} \langle |\delta E_y^{(\pm)}(x_f, z_f)|^2 \rangle\, r; \quad \text{for the air region} \tag{7}$$

$$\langle P^{(\pm)}(\theta) \rangle = \frac{n_3 k}{2\omega\mu} \langle |\delta E_y^{(\pm)}(x_f, z_f)|^2 \rangle\, r; \quad \text{for the substrate region} \tag{8}$$

where ω and μ are the angular frequency of light and the magnetic permeability in vacuum. Substituting (6) into (7) and (8), and using the correlation functions of (4), we can obtain the radiated power in the air and substrate regions and then plot the scattered light intensity as a function of the angle θ.

The important features of this theory are illustrated by the rectilinear plot as seen in Figs. 2-7. A number of parameters are chosen in order to match those of the present measurements and appeared in each figure: $N23(= n_2/n_3) = 1.0533$, $TL(= t/\lambda) = 2.9409$, and $TH0(= t \cdot h_0) = 2.7175$, h_0 being the propagation constant of the incident TE_0 mode at $\lambda = 0.633$ μm. These values correspond to a 7059 sputtered glass of film thickness $t = 1.86$ μm on a pyrex glass substrate of the index $n_3 = 1.470$. It should be noted that each curve with different parameters is scaled to be almost the same peak in intensity because the angular features of the scattered light intensity are required for comparison with the measurements. Among the important parameters of the theory are the correlation lengths in the directions parallel and normal to the waveguide. For simplicity, the correlation length of index fluctuations in the x direction is assumed to be equal to that of the surface roughness and to that of the cross correlation between them. The same assumption is taken in the z direction as well. These are described in a form normalized with λ as follows:

$$BXL(= b_x/\lambda) = AXL(= a_x/\lambda) = DXL(= d_x/\lambda)$$
$$BZL(= b_z/\lambda) = AZL(= a_z/\lambda) = DZL(= d_z/\lambda). \tag{9}$$

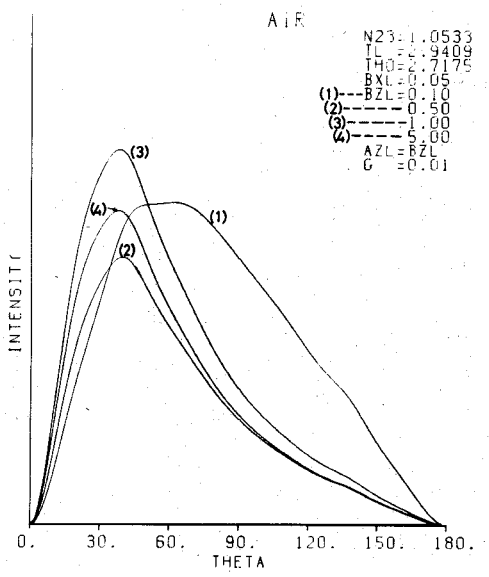

Fig. 2. Theoretically determined angular distribution of scattered light in the air region for $G = 0.01$.

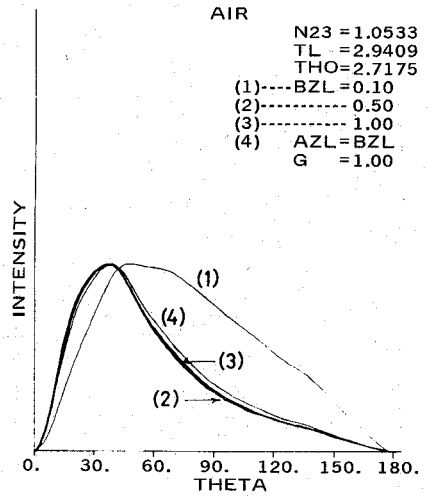

Fig. 3. Theoretically determined angular distribution of scattered light in the air region for $G = 1.0$.

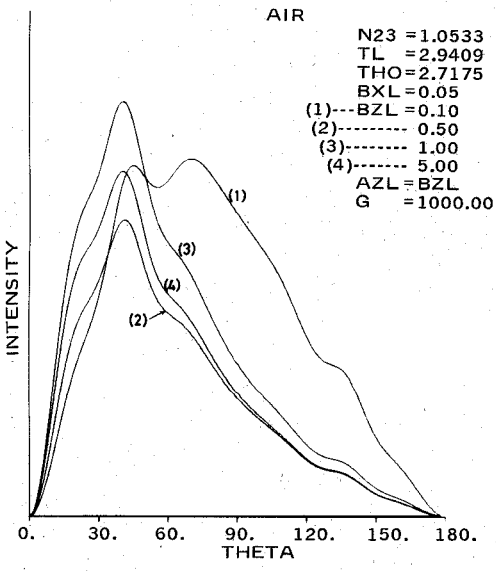

Fig. 4. Theoretically determined angular distribution of scattered light in the air region for $G = 1000$.

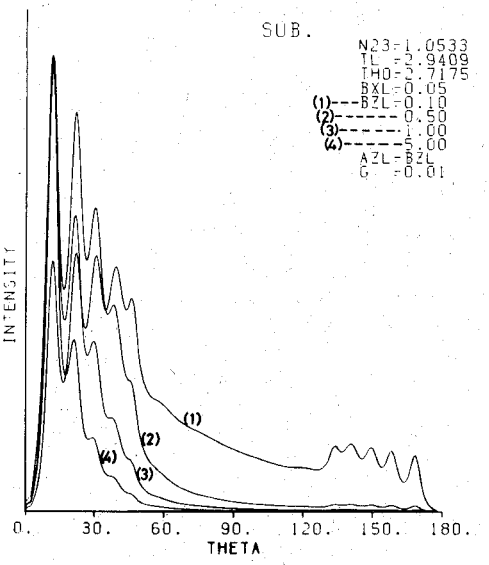

Fig. 5. Theoretically determined angular distribution of light scattering out of the substrate for $G = 0.01$.

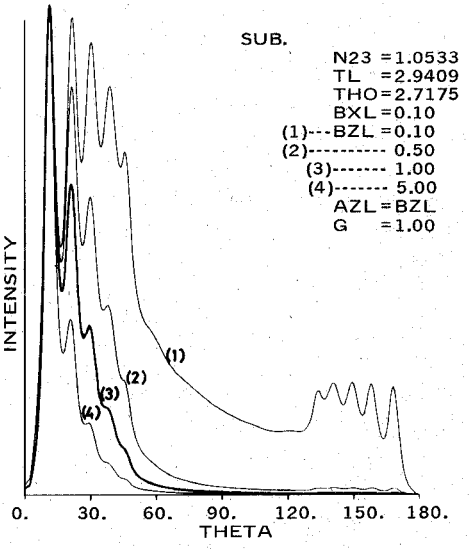

Fig. 6. Theoretically determined angular distribution of light scattering out of the substrate for $G = 1.0$.

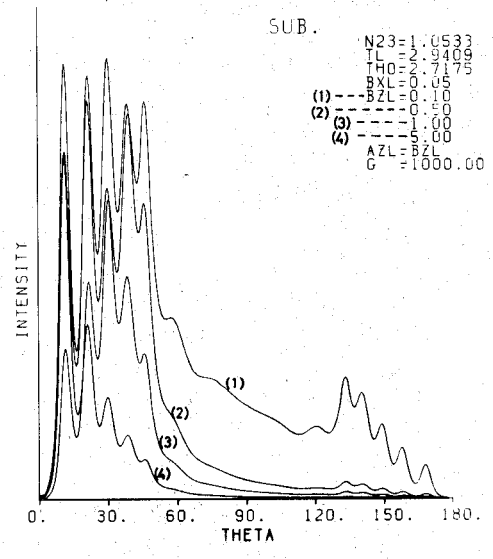

Fig. 7. Theoretically determined angular distribution of light scattering out of the substrate for $G = 1000$.

Another parameter which may influence the radiation patterns or scattered light is $G = V_f/(V\lambda)$. This is introduced to evaluate which imperfections more efficiently affect the size distributions, shapes, and other parameters of scattering data. Since G is proportional to the ratio V_f/V, for a relatively small value of $G = 0.01$ the scattered light intensity occurs mainly due to the refractive index inhomogeneities of the waveguide core, which are the cases of Figs. 2 and 5. For a large value of $G = 1000$, as shown in Figs. 4 and 7, the radiation patterns in the air and substrate regions are almost determined by scattered power caused by surface roughness of the waveguide wall. It can be seen in Figs. 2-4 that the air radiation takes a maximum at an angle about 40° regardless of G and BZL except for $BZL = 0.10$ and shifts to a lower angle with the increase of BZL. The air radiation directivity is also affected by BXL, the intensity peak for $BXL \gtrsim 1.0$ moves to the angle less than 35° in the forward quadrant, and has a narrower angular width. The substrate radiation is highly directional compared with the air radiation. The important differences between the air and substrate scattering patterns is that the substrate radiation is more peaked in the forward direction. The multiply intensity pattern may occur due to interference between the light scattered directly to the substrate region and that scattered indirectly after many reflections at film-air interfaces [6], [7]. The angular positions of multiple peak scatters remain essentially unchanged with the correlation length, but the ratio of main peak to other subsidiaries is lowered considerably with increasing BZL. With respect to the effect of G on the scattering patterns, the increase of the parameter allows the air radiation to become progressively peaked at about 70° as shown in Fig. 4. The distributions of scattered light intensity extend over the larger angle in the substrate scattering region as well. The extreme cases of G greater than 1000 or less than 0.01 does not change the gross features of angular patterns of light intensity. However, a remarkable difference in scattering patterns is observed when the parameter is ranged between $G = 1.0$ and 10.0. This suggests that the radiated power of light scattered out of the waveguide with bulk inhomogeneities alone is comparable to that of the waveguide with surface roughness, so that the resultant curve of scattering is complicated in a way that the scattered fields caused by both effects interfere each other [9]. When $G \ll 1.0$ or $G \gg 10.0$ for film thickness $t/\lambda = 2.9409$, the influence on the magnitude of the scattering due to cross correlation between both imperfections becomes relatively insensitive since the effect of bulk inhomogeneities is predominant much over that of surface roughness or vice versa.

III. Experiments and Discussion

The Corning 7059 glass thin film with a variety of thickness ranging from 1.0-13 μm are deposited by RF sputtering onto a pyrex glass substrate. The sample waveguides of different thickness are controlled through varying sputtering time, while argon pressure and RF input power are fixed during deposition of the waveguide film. The typical scattering loss measured is as relatively high as 3-4 dB/cm for TE_0 mode excitation, compared with the lowest values previously reported for sputtered glass thin-film waveguides [8]. The experimental setup used to measure the angular distribution of scattered light is shown in Fig. 8. The laser light from a He-Ne laser of $\lambda = 0.633$ μm is coupled to the thin film by means of a prism coupler with a short focal length lens. A polarizer is used to select the TE polarization of a light beam propagating in the waveguide. The surface of the waveguide is masked so that only 1 mm width of light beam from a selected region is visible. The scattered light from the masked waveguide is detected by use of a photomultiplier via a light guide to collect efficiently the weakly scattered light. The front end of the light guide is maintained to be about 6 cm apart from the waveguide surface, which ensures the theory of waveguide scattering developed in the preceding section. This fact allows us to detect scattered light in the far-field diffraction region. In order to enhance the directivity of the detector system, an aluminum tube (inner diameter 1 X 2 mm) is attached to the tip of the light guide. The detector system can be rotated in a plane normal to the guided beam. The rotating arm is motor-driven to scan an almost semicircle range in the air and substrate regions and the angular position is indicated on the x axis of an x-y recorder. The y axis is driven by the photomultiplier signal after suitable amplification using a lock-in-amplifier. The angular resolution of the whole detector system is about 3°, which is adequate for comparison with the theoretical curves [11]. For the scattered light of substrate radiation, the surface of the substrate glass is submerged in a bath filled with liquid paraffin of the index $n = 1.474$ to suppress the light reflected from the substrate-air interface. The detector circuit is thus rotated in the container as shown in Fig. 9. Since the refractive index of the liquid differs slightly from that of the pyrex glass, the error of angular dependence induced in the substrate radiation is estimated to be about 0.5° at $\theta = 15°$ or less at $\theta > 15°$. This is negligible compared with angular resolution of the rotating detector system.

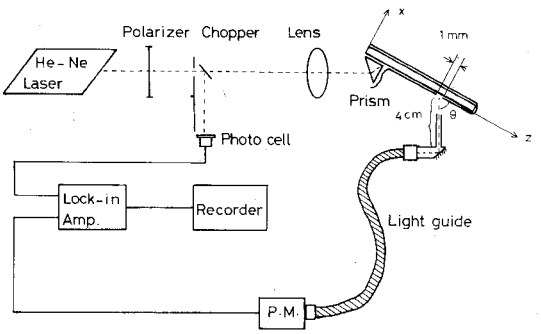

Fig. 8. Experimental setup to measure scattered light intensity.

Typical results of substrate radiation in an out-of-plane scattering are shown in the left-hand sides of Figs. 10-12 for sputtered glass films. The thin films, numbered $P14$, $P6$, and $P15$ were of widths of 1.09 μm, 1.86 μm, and 3.95 μm and of the respective refractive indexes of 1.554, 1.548, and 1.552, which were determined by prism coupling measurements. The refractive index of the waveguide $P6$ is found to be 0.3 percent lower than the other samples because of small process variations of argon pressure. The right-hand side of each figure represents the theoretical curves corresponding to the measured scattering patterns. The gross features of the measured curves are consistent with the theory taking account of both imperfections, assuming correlation lengths of $BXL = AXL = DXL =$

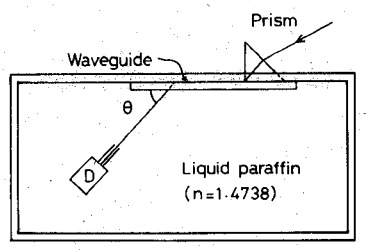

Fig. 9. The container is filled with liquid paraffin in which detector (D) is rotated.

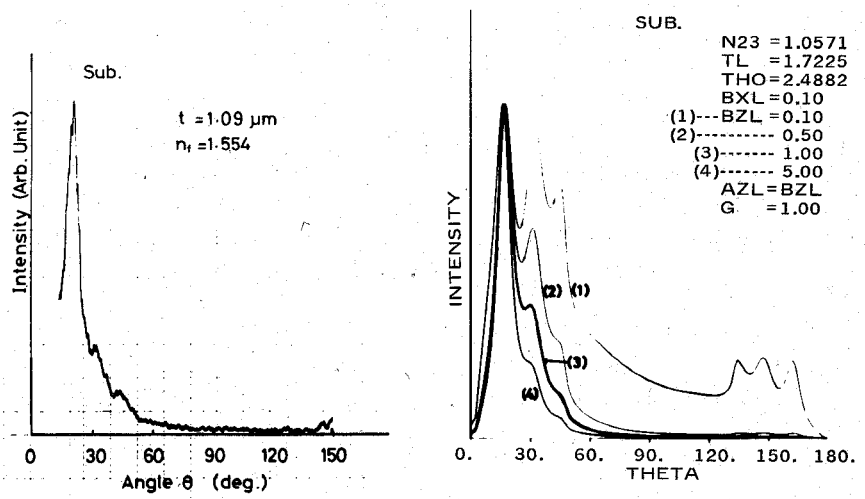

Fig. 10. Measured scattering curve of the substrate radiation (left-hand side) and theoretically determined curves matching those of the measurement (right-hand side) for waveguide $P14$.

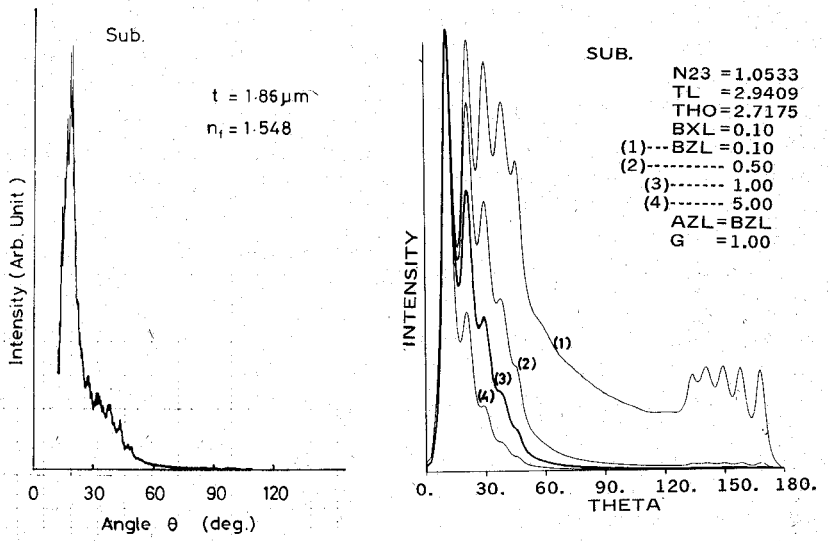

Fig. 11. Measured scattering curve of the substrate radiation (left-hand side) and theoretically determined curves matching those of the measurement (right-hand side) for waveguide $P6$.

0.1 and $BZL = AZL = DZL = 1.0$. Another parameter which is easily compared with the experiments is the ratio G, which is reasonably estimated to range between 1.0 and 5.0. The substrate radiation patterns, drawn by boldface, then bear a close resemblance to the measured curves as can be seen in the figures. For the sample $P6$, the scattered light peaks predominantly at $\theta = 16^\circ$ in the forward substrate direction, which is also in good agreement with the theoretical curve. The locations of multiple peak scatters correspond fairly to the measured data. But the considerably lower magnitudes of the peak intensities are observed in Fig. 11. The measured scattering curve of Fig. 10 behaves similarly to that of Fig. 11. The substrate radiation is highly peaked at $\theta = 20^\circ$, and accompanied with multiple scattered intensities between 30° and 50°. On the other hand, for a thick waveguide of the sample number $P15$ the main peak that is expected at the angle lower than 10° is not observed because of mechanical limitation of the apparatus, whereas the second and third peaks of

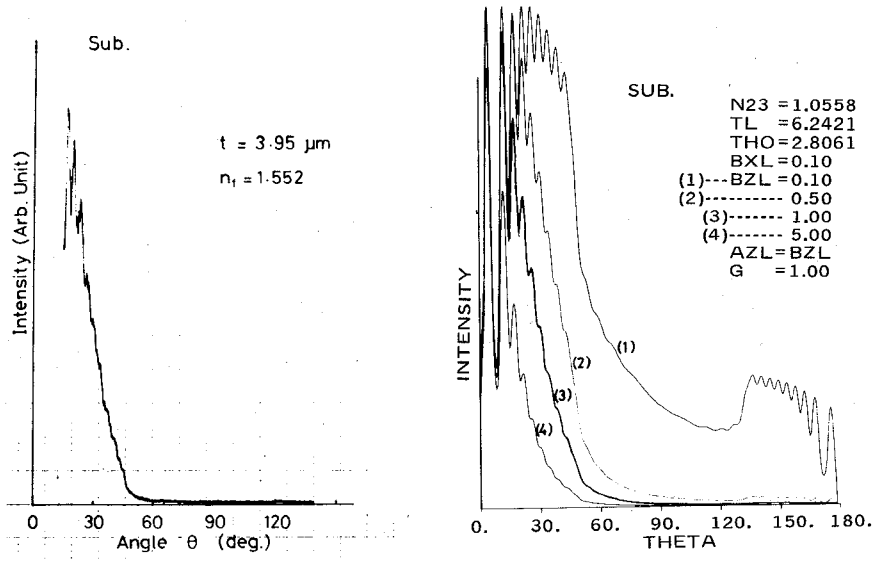

Fig. 12. Measured scattering curve of the substrate radiation (left-hand side) and theoretically determined curves matching those of the measurement (right-hand side) for waveguide $P15$.

the subsidiaries are at least consistent with the theoretical curve with parameters chosen above. The fine structures in the substrate scattering become progressively more condensed as the thickness of the glass film increases. The general features of radiation patterns, however, will not change by the fluctuating components since the property of the angular dependence of scattered light intensity relies on the inhomogeneities of an imperfect waveguide.

The scattering pattern measurements on air radiation are also done, although the measured data are not presented graphically. It can be seen that the air radiation patterns exhibit a broad directivity as expected from Fig. 3. Actually, scattered intensity peaked at 40° with an angular width larger than 40°, which is consistent with the theoretical prediction assuming the parameters chosen for the substrate radiation [11]. In the measured intensity of the sample waveguide $P14$, the separated peaks appeared in the forward quadrant of the air radiation. These are of very high intensity compared with the background, and can be easily discerned from its uniform appearance of the background scatters. This may result from the presence of dust particles during the deposition of the thin film, or possibly during the cleaning procedure [8]. From these observations of scattering patterns, the theory of waveguide imperfections is found to be applicable to both cases of the air and substrate radiations, taking the parameters of $BXL = 0.1$, $BZL = 1.0$, and $G = 1.0$ into account. The estimated value of G suggests that the effects of waveguide surface roughness and bulk inhomogeneities of the waveguide core contribute equally to radiated power of scattering [9]. The scattering theory based on mutual correlation between the waveguide imperfections allows us to conclude that the standard deviation of surface roughness leads to $V_f = 6$ Å at $G = 1.0$ and $V_f = 32$ Å at $G = 5.0$ when $V = 1 \times 10^{-3}$ is assumed, that is, when the index fluctuation of the waveguide core is taken as the order of 0.1 percent. This is a reasonable expectation for the rms deviation of the irregular boundaries since the values are compared favorably to the previously reported ones [2], [4] in which the scattering loss is caused by the imperfections of the surface roughness alone.

IV. Conclusions

The radiation patterns from optical waveguides prepared by sputtering 7059 glass onto pyrex glass substrates are greatly affected by surface preparation and sputtering conditions. The angular dependence of the air and substrate scatterings may be related to the structures involved in the waveguide. In order to examine this, the experimental data were compared with the theory based on scattering from surface roughness and bulk inhomogeneities of the waveguide core. We find very good agreement with the present analysis assuming the proper correlation lengths and rms values for these parameters. The results obtained may be useful in optimizing the fabrication procedures and reducing the scattering loss to a minimum possible value in the sputtered glass waveguide. Scattering from indiffused waveguides such as potassium ion exchange in a soda-lime glass, whose type of the optical waveguide is also important in integrated optics, is different in origin and will be reported later.

Acknowledgment

The authors would like to thank S. Miyanaga for his help in preparing theoretically calculated scattering patterns.

References

[1] J. T. Boyd and D. B. Anderson, "Effect of waveguide optical scattering on the integrated optical spectrum analyzer dynamic range," *IEEE J. Quantum Electron.*, vol. QE-14, pp. 437–443, June 1978.

[2] D. Marcuse, "Mode conversion caused by surface imperfections of a dielectric slab waveguide," *Bell Syst. Tech. J.*, vol. 48, pp. 3187–3215, Dec. 1969.

[3] —, "Power distribution and radiation losses in multimode dielectric slab waveguides," *Bell Syst. Tech. J.*, vol. 51, pp. 429–454, Feb. 1972.

[4] Y. Suematsu, K. Furuya, M. Hakuta, and K. Chiba, "Far-field radiation pattern caused by random wall distortion of dielectric waveguides and determination of correlation length" (in Japanese), *Trans. IECE Japan*, vol. 56-C, pp. 377–384, July 1973.

[5] J. Nayyer, Y. Suematsu, and H. Tokiwa, "Mode coupling and radiation loss of clad-type optical waveguides due to the index inhomogeneities of the core material," *Opt. Quantum Electron.*, vol. 7, pp. 481–492, 1975.

[6] M. Imai, S. Miyanaga, and T. Asakura, "Mode conversion and radiation loss caused by refractive-index fluctuations in an

asymmetric slab waveguide," *IEEE J. Quantum Electron.*, vol. QE-13, pp. 255-262, Apr. 1977.
[7] S. Miyanaga, M. Imai, and T. Asakura, "Radiation pattern of light scattering from the core region of dielectric-slab-optical waveguides," *IEEE J. Quantum Electron.*, vol. QE-14, pp. 30-37, Jan. 1978.
[8] M. Gottlieb, G. B. Brandt, and J. J. Conroy, "Out-of-plane scattering in optical waveguides," *IEEE Trans. Circuits Syst.*, vol. CAS-26, pp. 1029-1035, Dec. 1979.
[9] S. Miyanaga, T. Asakura, and M. Imai, "Scattering characteristics of a beam mode in dielectric-slab optical waveguide," *Opt. Quantum Electron.*, vol. 11, pp. 205-215, 1979; —, "Scattering characteristics of a beam mode in a dielectric-slab optical waveguide. Part II," *Opt. Quantum Electron.*, vol. 12, pp. 23-33, 1980.
[10] D. Marcuse, *Theory of Dielectric Optical Waveguides*. New York: Academic, 1974, ch. 1.
[11] M. Imai, M. Koseki, and Y. Ohtsuka, "Light scattering from a glass thin-film optical waveguide," *J. Appl. Phys.*, vol. 52, pp. 6506-6508, Nov. 1981.

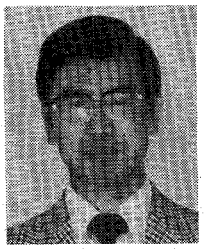

Masaaki Imai (S'67-M'69) received the B.E., M.E., and D.E. degrees in electronic engineering from Hokkaido University, Sapporo, Japan, in 1964, 1966, and 1969, respectively.

He was a Research Associate at the Research Institute of Applied Electricity, Hokkaido University, from 1969 to 1977 and during the academic years of 1972-1974, and was also a visiting Research Fellow at the Communications Research Centre, Ottawa, Canada. He is presently an Associate Professor at the Department of Engineering Science, Faculty of Engineering, Hokkaido University. His research interests include integrated optics, fiber optics, and the application of fiber technology to communications and sensors.

Dr. Imai is a member of the Optical Society of America, the Institute of Electronics and Communication Engineers of Japan, and the Japan Society of Applied Physics.

Yoshihiro Ohtsuka was born in Chiba, Japan, on April 29, 1934. He graduated from Defence Academy, Yokosuka, Kanagawa, Japan, in 1959. After two years at the Japan Defence Agency, he became a graduate student in applied physics at Osaka University, Osaka, Japan, and received the M.E. and D.E. degrees in 1964 and 1968, respectively.

He was a Research Associate at the Department of Applied Physics, Faculty of Engineering, Osaka University, from 1964 to 1968, and also a member of the research fellows at the Institute of Plasma Physics, Nagoya University, from 1966 to 1968. In 1968 he was promoted to an Associate Professor at the Department of Engineering Science, Faculty of Engineering, Hokkaido University, Sapporo, Japan. From 1974 to 1975 he was with the research group on fiber optics at the Department of Electronics, University of Southampton, Southampton, England. Since 1977, he has been Professor of Engineering Science at Hokkaido University and is working in optics related to laser physics and its applications.

Dr. Ohtsuka is a member of the Optical Society of America and the Japan Society of Applied Physics.

Mamoru Koseki received the B.E. and M.E. degrees in applied physics from Hokkaido University, Sapporo, Japan, in 1978 and 1981, respectively.

He is now with the Totsuka Works, Hitachi Limited, Yokohama, Japan. When he was working towards the M.E. degree he was engaged in optical waveguide fabrication techniques and measurements.

Mr. Koseki is a member of the Japan Society of Applied Physics.

GaAs/GaAlAs Curved Rib Waveguides

MICHAEL W. AUSTIN

Abstract—**Curved dielectric optical waveguides suffer from radiation loss due to bending. To minimize the bending loss and reduce the radius of curvature, it is necessary to fabricate guides which provide strong optical confinement. This paper gives a brief review of curved waveguide analysis and presents some experimentally measured loss values for GaAs/GaAlAs curved rib waveguides. The rib waveguides, fabricated using ion beam milling, have a large rib height and are tightly guided structures. When corrected for reflection losses and input coupling efficiency, a minimum loss of approximately 3 dB has been achieved for a multimode 90° curved guide with a radius of curvature of 300 μm, and 8.5 dB for a single-mode curved guide with a radius of curvature of 400 μm. It is believed that most of this residual loss is not radiation loss due to bending, but rather scattering loss due to rib wall imperfections.**

Manuscript received September 25, 1981; revised October 19, 1981.

The author is with the British Telecom Research Laboratories, Ipswich, England.

INTRODUCTION

MANY devices likely to be incorporated in integrated optical circuits, such as directional couplers, Y-couplers, and switches may require sections of curved optical waveguide and it will also be necessary to use curved waveguides in order to increase the device packing density in these circuits. In addition to the loss mechanisms present in straight waveguides, such as absorption and scattering, curved dielectric guides suffer from radiation loss due to bending [1]. This bending loss may be very large if the guide is bent abruptly. Several authors [1]-[11] have investigated the problem of continuous radiation from curved dielectric waveguides, but very few curved guides have been fabricated [12]-[16]. The guides that have been made were in either sputtered glass films on glass substrates

0018-9480/82/0400-0641$00.75